



Surface Tension and Viscosity of Binary Mixtures of the Fluorinated and Non-fluorinated Ionic Liquids [PFBMIm][PF₆] and [C₄C₁Im][PF₆] by the Pendant Drop Method and Surface Light Scattering

Thomas M. Koller, et al. *[full author details at the end of the article]*

Received: 19 June 2020 / Accepted: 18 July 2020 / Published online: 12 August 2020
© The Author(s) 2020

Abstract

Mixtures of fluorinated and non-fluorinated ionic liquids (ILs) show a distinct structural organization in the bulk and at the surface. To understand how such microscopic effects influence the macroscopic bulk and surface properties of IL mixtures, knowledge of corresponding thermophysical properties including viscosity and surface tension is required yet lacking. With the intention of investigating surface enrichment effects of the fluorinated IL [PFBMIm][PF₆] (3-methyl-1-(3,3,4,4,4-pentafluorobutyl)imidazolium hexafluorophosphate) in mixtures with the structurally similar, non-fluorinated IL [C₄C₁Im][PF₆] (1-butyl-3-methylimidazolium hexafluorophosphate) observed with angle-resolved X-ray photoelectron spectroscopy (ARXPS), the pendant drop method and surface light scattering (SLS) were applied in the present study to determine surface tension and dynamic viscosity between (293 and 368) K. By adding small amounts of [PFBMIm][PF₆] up to 9 mol %, a distinct increase in the viscosity and decrease in the surface tension of the mixtures relative to the properties of pure [C₄C₁Im][PF₆] was found. This behavior reflects the nanosegregated structure in the bulk and at the surface of the binary IL mixtures. Using the results about the pronounced surface enrichment of the fluorinated chain of [PFBMIm][PF₆] quantified by ARXPS, a linear mixing rule for the surface tension of the IL mixtures based on the surface tensions of the pure ILs and the surface concentration of their most surface-active groups is suggested.

Keywords Ionic liquids · Mixtures · Pendant drop method · Surface light scattering · Surface tension · Viscosity

Electronic supplementary material The online version of this article (<https://doi.org/10.1007/s10765-020-02720-w>) contains supplementary material, which is available to authorized users.

1 Introduction

Ionic liquids (ILs) are interesting working fluids in different fields of chemistry and engineering such as electrolysis [1, 2], catalysis [3, 4], or separation technology [5, 6]. Often, ILs consist of an inorganic anion and an organic cation with at least one alkyl chain of varying length attached to the charged head group of the cation [7]. Within the last years, ILs featuring fluorinated alkyl chains in the anion or cation, so-called fluorinated ILs, received considerable attention due to their, for example, high chemical stabilities and large solubilities for gases [8, 9]. By using, *e.g.*, mixtures of fluorinated and non-fluorinated ILs, their properties can be tailored for specific applications [10–12]. Therefore, it is necessary to know the thermophysical properties associated with the bulk and the surface of such IL mixtures. In this study, the viscosity and especially the surface tension as representative bulk and surface properties are of main interest. The viscosity as one key transport property describes momentum transfer [13] and the surface tension is relevant in connection with, for example, mass transport across phase boundaries and wetting [14].

To represent thermophysical properties of IL mixtures, experiments, simulations, and theoretical approaches have been used; see, *e.g.*, Refs. [10, 11, 15]. In this connection, reliable data obtained from measurement techniques of proven validity are inevitable to validate and develop molecular simulations [16, 17] and to establish prediction schemes [12, 16, 18]. Experimental thermophysical property research on IL mixtures is strongly focused on their phase equilibria including melting points and densities [15, 19–24], while viscosity [15, 19, 21, 22, 24] and in particular surface tension [12, 25–27] have been studied to much lesser extent. In most cases related to fluorinated ILs, only the pure fluids featuring fluorinated chains, in the anion rather than in the cation, were investigated with respect to viscosity and surface tension [8, 9, 28, 29]. For these two properties, only a single study on binary mixtures of fluorinated and non-fluorinated ILs with a common anion is given by Merrigan *et al.* [25]. By adding 0.3 mass % of four different fluorinated ILs to a non-fluorinated IL, a decrease in the surface tensions of the corresponding binary IL mixtures ranging between (10 and 15) % relative to the value of the non-fluorinated IL was reported [25].

For binary mixtures of non-fluorinated ILs, the viscosity [10, 11, 15] and surface tension [12, 26] often show a distinct non-ideal behavior as a function of composition. This is reflected in deviations of the experimental data from linear mixing rules. Deviations are found especially for the surface tension as the surface-near region can show a composition which is significantly different from that in the bulk [12, 30]. Though very speculative, it is common practice that thermophysical property data of ILs or IL mixtures are used to draw conclusions about the fluid structure. Vice versa, the macroscopic thermophysical properties are governed by the molecular interactions, resulting from a specific fluid structure on a microscopic level [10, 12, 31].

Owing to the different types of interactions present [7, 10], ILs exhibit a highly organized “nanostructure” in the bulk and at the surface. For non-fluorinated

ILs, the liquid bulk features polar nanodomains consisting of the anion and the cationic head group as well as nonpolar ones made up of sufficiently long alkyl chains [10, 31]. The latter are preferentially enriched at the IL surface given their relatively low cohesive energy [10, 16, 32]. By including fluorinated chains in the anions or cations of pure ILs, experiments [30, 33] and molecular dynamics (MD) simulations [9, 17, 28] showed that the bulk and surface characteristics are altered. In the liquid bulk, the polar and nonpolar colloid-like domains are accompanied by nonpolar “fluorous” domains containing the fluorinated chains [9, 28, 33]. At the surface, a competition between the nonpolar alkyl chains in the cation and the fluorinated chains in the anion was observed [17]. For relatively short alkyl chains, the outer surface is preferentially occupied by the fluorinated chains, while the latter are gradually replaced by alkyl chains with increasing chain length [17].

To investigate whether such surface enrichment effects are also present in mixtures of fluorinated and non-fluorinated ILs, Heller *et al.* [30] have recently applied angle-resolved X-ray photoelectron spectroscopy (ARXPS). With this method, the composition and molecular arrangement at the surface-near region with an information depth of about (1.0 to 1.5) nm can be analyzed under ultra-high vacuum conditions; see, *e.g.*, Refs. [30, 34–36]. For binary mixtures of the non-fluorinated IL [C₄C₁Im][PF₆] (1-butyl-3-methylimidazolium hexafluorophosphate) and the structurally similar fluorinated IL [PFBMIm][PF₆] (3-methyl-1-(3,3,4,4,4-pentafluorobutyl)imidazolium hexafluorophosphate) with a partial fluorination in the cationic alkyl chain, a pronounced enrichment of the fluorinated chain at the surface was observed [30], which is in accordance with the aforementioned findings for pure ILs [17] and with those reported for another binary mixture of fluorinated and non-fluorinated ILs [12]. The predominant surface presence of the fluorinated chain, being more distinct with decreasing [PFBMIm][PF₆] content, was associated with the lower surface tension of the fluorinated IL than of the non-fluorinated IL [30], an assumption that has not yet been proven experimentally.

Motivated by the aforementioned structural effects observed for IL systems containing fluorinated and non-fluorinated alkyl chains, our interest within the present work was directed to the question to which extent such effects influence the surface tension and viscosity of binary mixtures of fluorinated and non-fluorinated ILs. For answering this question, binary mixtures of the ILs [PFBMIm][PF₆] and [C₄C₁Im][PF₆] were selected as model system for the experimental investigation by surface light scattering (SLS) and the pendant drop (PD) method under consistent conditions at macroscopic thermodynamic equilibrium. Here, the surface tension data obtained from the analysis of the contour of pendant drops were combined with information about the dynamics of surface fluctuations probed by SLS in order to determine the viscosity of the bulk phase. For evaluating the measurement results from both techniques relying on rigorous working equations, also density measurements were performed. To probe whether the observed surface enrichment effects are reflected in the surface tension data and in the dynamics of the surface fluctuations, we focused on the influence of small amounts of [PFBMIm][PF₆] up to 9 mol % on the surface tension and viscosity of the IL mixtures between (293 and 368) K. Based on a discussion of the

thermophysical properties in connection with the detailed structural information available by ARXPS, a new strategy for relating the surface tension with the surface composition of the binary IL mixtures is proposed.

2 Experimental

2.1 Materials and Sample Preparation

The non-fluorinated IL $[\text{C}_4\text{C}_1\text{Im}][\text{PF}_6]$ (molecular weight $M=284.19 \text{ g mol}^{-1}$, melting temperature $T_m \approx 265 \text{ K}$) was purchased from IoLiTec with a specified mole fraction purity of 0.995. For the fluorinated IL $[\text{PFBMIm}][\text{PF}_6]$ ($M=374.14 \text{ g mol}^{-1}$, $T_m \approx 339 \text{ K}$), the synthesis of the sample with an estimated mole fraction purity of about 0.990 can be found in Ref. [37]. To remove particulate contaminations from the pure IL samples, syringe filters consisting of poly(tetrafluoroethylene) and having a pore size of 450 nm were applied at temperatures of (298 and 353) K for $[\text{C}_4\text{C}_1\text{Im}][\text{PF}_6]$ and $[\text{PFBMIm}][\text{PF}_6]$. Binary IL mixtures with a focus on relatively low mole fractions of the fluorinated IL $[\text{PFBMIm}][\text{PF}_6]$ in the bulk, $x_{\text{F,B}}$, with values of about 0.03 and 0.09 were made. For the smaller of the two compositions, two different samples with similar contents of $x_{\text{F,B}}=0.028$ and 0.029 were prepared for investigations with the different techniques requiring different sample amounts, as it is discussed in the Supplementary Material. For the mixture preparation, the corresponding IL masses were added to flasks and weighed with a balance (Sartorius Entris 224i-1S) with an expanded uncertainty on a 95 % confidence level (coverage factor $k=2$) of 1 mg. Considering the weighing procedure, the absolute uncertainty ($k=2$) in the mole fractions $x_{\text{F,B}}$ of the binary mixtures can be estimated to be 0.001.

For reducing the amount of water or other volatile compounds, all samples were then degassed by an oil-sealed vacuum pump over a period of 3 h at temperatures above the melting point of the samples and at a pressure of 10^{-5} MPa. For sample transfer and handling and as inert gas in the sample cells, argon purchased from Linde AG with a mole fraction purity of 0.99999 was used. Except for the pure $[\text{PFBMIm}][\text{PF}_6]$, the concentration of water by mass, $w_{\text{H}_2\text{O}}$, was determined by Karl Fischer coulometric titration (Metrohm, 756 KF coulometer) before and after the experiments and averaged. For all water contents with an estimated relative expanded uncertainty ($k=2$) of 10 %, average values ranging between $9.8 \cdot 10^{-4}$ and $1.8 \cdot 10^{-3}$ were obtained. This can be considered to be sufficiently small enough to have no impact on the properties of the IL samples [38]. Detailed information about the sources, purities, and compositions of the samples investigated is given in Table 1.

Example IL samples investigated in this work have been analyzed in ARXPS measurements concerning their purity. Within the error margins, the results matched the previous measurements reported by Heller *et al.* [30]. Thus, the structural results detailed therein can reliably be discussed in connection with the present investigations.

Table 1 Specification of the investigated IL samples

IL samples	Source	Mole fraction purity	Mole fraction $x_{F,B}$ of [PFBMIm][PF ₆]	Water mass fraction $w_{H_2O}^b$
[C ₄ C ₁ Im][PF ₆]	IoLiTec	0.995	0	$1.3 \cdot 10^{-3}$
[C ₄ C ₁ Im][PF ₆] + [PFBMIm][PF ₆]	–	–	0.028 ^a	$9.8 \cdot 10^{-4}$
[C ₄ C ₁ Im][PF ₆] + [PFBMIm][PF ₆]	–	–	0.029 ^a	$9.8 \cdot 10^{-4}$
[C ₄ C ₁ Im][PF ₆] + [PFBMIm][PF ₆]	–	–	0.090 ^a	$1.8 \cdot 10^{-3}$
[PFBMIm][PF ₆]	Synthesis	0.990	1	–

^aThe expanded uncertainty $U_c(k=2)$ for the mole fraction is $U_c(x_{F,B})=0.001$

^bThe expanded relative uncertainty $U_r(k=2)$ of the water content obtained by Fischer coulometric titration is $U_r(w_{H_2O})=10\%$

2.2 Vibrating-Tube Densimeter

The liquid density ρ required for the evaluation of the PD and SLS experiments was measured at atmospheric pressure of 0.1 MPa with the vibrating-tube densimeter models DMA 5000 M and DMA 5000 from Anton Paar. The DMA 5000 M was used for the pure [C₄C₁Im][PF₆] and for its mixture with a [PFBMIm][PF₆] mole fraction of 0.028 at temperatures between (293 and 363) K in steps of 5 K. For the pure [PFBMIm][PF₆] with a relatively large melting point of 339 K, the DMA 5000 instrument was applied between (340.65 and 363.15) K in steps of 2.5 K. For further details on the adjustment and measurement procedures, the measurement results, and the uncertainties of the density data, the reader is referred to the Supplementary Material.

2.3 Pendant Drop (PD) Method

The surface tension σ of the pure ILs and their mixtures in an argon atmosphere at about 0.11 MPa was measured by the PD method. Although the term surface tension is only connected to pure fluids consisting of a liquid and a vapor phase under saturation conditions, it is also employed for all investigated systems in the following for the sake of convenience. Besides being the key property for analyzing the effects of an enrichment of [PFBMIm][PF₆] at the liquid surface in mixtures with [C₄C₁Im][PF₆], the surface tension is also required to evaluate the SLS measurements with respect to viscosity in the present case of overdamped surface fluctuations. The PD method relies on the evaluation of the contour of a pendant drop based on the Young–Laplace equation. This equation describes the profile of axisymmetric fluid bodies, such as bubbles or droplets, that are immersed in another fluid, are exposed to a gravitational field, and form a stable phase boundary [14]. In connection with the measurements for pure [C₄C₁Im][PF₆] and [PFBMIm][PF₆] as well as their mixtures at mole fractions of 0.029 and 0.090 of the fluorinated IL for temperatures between (298 and 368) K, the corresponding details on the measurement procedures

and conditions are reported in the Supplementary Material. In the following, the evaluation of the surface tension data of the IL samples is described.

The calibration of the pictures with respect to the transition from the pixel to the metric scale was realized by the outer diameter of the capillary. For this, the diameter of the capillary tip visible in the pictures was measured several times with a caliper, resulting in an average value of 1.57 mm. Here, the expanded ($k=2$) uncertainty is 0.03 mm, which corresponds to a relative expanded uncertainty of 1.91 %. In the analysis of the recorded pictures of the pendant drops, the Canny edge detector [39] was used to identify the droplet contour. To find suitable start values for the numerical solution of the Young–Laplace equation, the radius of a circle representing the curvature of the drop shape at the apex was estimated with a circle fit function [40]. This radius was combined with the approximation of the Bond number as given by Hansen *et al.* [41] and the Young–Laplace equation to estimate the surface tension of the system studied. Here, the middle of all pixels representing the lower edge of the droplet picture is assumed to be the horizontal position of the apex. For applying the Bond number approximation, the maximum width of the droplet and the droplet width at the vertical distance from the apex being equal to the maximum droplet width were determined from the detected droplet contour. In this and in the further evaluation steps, the acceleration of gravity $g=9.81 \text{ m}\cdot\text{s}^{-2}$ and the densities of the liquid and the surrounding gas phase are needed.

To determine the final surface tension value for a given droplet picture, theoretical drop profiles were compared to the experimental one. For generating suitable theoretical drop profiles, the Young–Laplace equation was solved numerically by using the 4th order Runge–Kutta algorithm. Here, the radius representing the curvature at the apex and the surface tension value are varied independently within limited intervals around the approximation results obtained by the procedure described above. The corresponding grid featured total ranges and step sizes of (10 and 0.13) pixels for the radius representing the curvature at the apex and (8 and 0.1) $\text{mN}\cdot\text{m}^{-1}$ for σ . For each combination, the deviation of the theoretical drop profile from the experimental one was calculated considering all contour points up to the droplet height being equal to the maximum droplet diameter. Here, the theoretical drop profiles were also shifted horizontally and vertically within ± 0.5 pixels in steps of 0.25 pixels relative to the experimental profile to account for any errors of the apex location determined from the droplet contour. The surface tension in the theoretical parameter set, which represented the experimental drop profile best, was considered to be the correct one. The σ values listed in the Supplementary Material are the averages of the 3 to 5 droplets analyzed for each state. Repetition measurements performed for the mixture with $x_{\text{F,B}}=0.090$ at (338 and 299) K agreed with the initial results clearly within the expanded ($k=2$) uncertainties of the surface tension data of 4 %. Furthermore, the maximum and average absolute relative deviations of the σ data obtained for the individual droplets from the reported mean values were (0.96 and 0.31) %.

Before the experiments for the IL systems, validation measurements were performed for deionized and degassed water as well as for *n*-dodecane in argon atmosphere at 303 K and compared with reference data. For the data evaluation, the densities of water and *n*-dodecane based on the publications of Wagner and Pruss [42] as

well as Lemmon and Huber [43] were extracted from the REFPROP database [44]. The same holds for the reference values for the surface tension. The measured values for water and *n*-dodecane of $(69.2 \pm 0.2$ and $23.5 \pm 0.2)$ mN·m⁻¹ showing larger and smaller σ values than the studied ILs deviated by $(-2.7$ and $-3.8)$ % from the reference values [45, 46]. Thus, the expanded ($k=2$) uncertainties of the surface tension data for the IL systems are estimated to be 4 %. This value is considered to reflect reasonably the two main uncertainty contributions attributable to the calibration procedure and the evaluation of the droplet profile.

For the evaluation of the pendant drops of the IL systems, the correlation of our experimental density data according to Eq. 2 with the parameters given in Table 2 were used assuming negligible solubility of argon in the ILs. As the density data were not measured for exactly the same mixture compositions studied with the PD method, ideal mixing of the pure ILs was assumed to calculate the corresponding mixture densities. This includes an extrapolation of the liquid density of [PFBMIm][PF₆] to temperatures below its melting point. Given that densities based on the ideal mixing rule do not deviate by more than 0.07 % from those measured for the mixture with a [PFBMIm][PF₆] mole fraction of 0.028, the impact of this simplification on the resulting σ data is assumed to be negligible. For the density of the argon atmosphere, the equation of state of Tegeler *et al.* [47] implemented in the REFPROP database [44] was employed at 0.11 MPa assuming that the vapor pressure of the ILs can be neglected. The uncertainties related to the assumptions made in the determination of density data for the evaluation of the PD experiments should be covered by the conservative estimation of the uncertainty of the obtained surface tension values.

2.4 Surface Light Scattering

With surface light scattering (SLS), the dynamics of thermal surface fluctuations present at the phase boundary of fluid systems is analyzed. In detail, the dynamics in the form of the frequency ω_q and damping Γ probed at a defined modulus of scattering vector q , *i.e.*, at a defined wavelength of the surface fluctuations is reflected by the temporal behavior of the scattered light emerging from the interaction of the incident laser light and the fluctuating surface [48, 49]. For fluids with relatively small viscosities and/or large surface or interfacial tensions, an oscillatory behavior of surface fluctuations is found by examining typically investigated wavelengths of

Table 2 Coefficients of Eq. 2 for the liquid density $\rho_{\text{calc}}(T)$ of the investigated IL systems at 0.1 MPa

System	$x_{\text{F,B}}$	$\rho_0/(\text{kg}\cdot\text{m}^{-3})$	$\rho_1/(\text{kg}\cdot\text{m}^{-3}\text{K}^{-1})$	$\rho_2/(\text{kg}\cdot\text{m}^{-3}\cdot\text{K}^{-2})$	AAD/ % ^a
[C ₄ C ₁ Im][PF ₆]	0	1649.24	-1.04824	3.45053×10^{-4}	0.0005
[C ₄ C ₁ Im][PF ₆] + [PFBMIm][PF ₆]	0.028 ± 0.001	1658.25	-1.05163	3.41808×10^{-4}	0.0005
[PFBMIm][PF ₆]	1	2262.28	-2.87060	2.70216×10^{-3}	0.0018

^aAverage absolute relative deviation between ρ and the correlation based on Eq. 2

fluctuations below about $10\ \mu\text{m}$ [48–50]. This enables a simultaneous determination of viscosity and surface tension by SLS [48, 50–54]. Fluids with relatively large viscosities and/or small surface or interfacial tensions show an overdamped behavior of surface fluctuations ($\omega_q=0$) [48, 49], which holds also for all present measurements. In this case, the accessible mean lifetime of surface fluctuations, $\tau_C=1/\Gamma\approx 2\eta/(\sigma q)$, is connected to the dynamic viscosity η and surface tension σ at a first approximation [48, 55, 56] and is of interest in this work. Here, combining the information about τ_C with the surface tension data obtained by the PD method also enabled to evaluate the viscosity of the true bulk phase. The latter property is accessed since the penetration depth of the surface fluctuations being on the order of μm is distinctly larger than the dimension of the surface-near region, where surface enrichment is found and which exhibits extensions on the order of 1 nm or less. For both the overdamped and oscillatory cases, the SLS technique represents an absolute method requiring no calibration procedure [48] and is based on rigorous working equations for the description of the dynamics of hydrodynamic surface fluctuations [57, 58].

For details about the fundamentals and methodological principles of the SLS technique, specialized literature [48, 49, 57, 58] is recommended. The SLS setup used in this work is the same as in our former investigations of systems consisting of a vapor and liquid phase including ILs [48, 51, 52, 55, 59]. Experimental procedures and conditions for the present measurements for pure $[\text{C}_4\text{C}_1\text{Im}][\text{PF}_6]$ and its binary mixtures with $[\text{PFBMIm}][\text{PF}_6]$ mole fractions of 0.028 and 0.090 at (293, 308, 338, and 368) K are described in the Supplementary Material. In the following, only measurement examples and the data evaluation relevant for this work is shown.

Within the present study, heterodyne conditions, where stronger reference light is superimposed to the light scattered at the phase boundary, and a sufficient suppression of line broadening effects are fulfilled. In this case, the normalized intensity correlation function for the analysis of overdamped surface fluctuations of a defined q value takes the form [48]:

$$g^{(2)}(\tau) = a + b \exp(-|\tau|/\tau_C). \quad (1)$$

In Eq. 1, the parameters a and b depend on the experimental boundary conditions. Besides the exponentially decaying mode with the characteristic decay time τ_C , in theory a second such mode with a shorter decay time and negative contribution to $g^{(2)}(\tau)$ is present [48]. Due to the typically much smaller signal strength of this second mode compared to the one shown in Eq. 1, this mode can usually not be resolved, which is also the case for the present measurements.

Figure 1 shows three example normalized pseudo-cross correlation functions of the scattered light intensity obtained for the three studied IL samples with $[\text{PFBMIm}][\text{PF}_6]$ mole fractions of $x_{\text{F,B}}=0, 0.028,$ and 0.090 at $T=308.22\ \text{K}$ and at a defined incident angle $\Theta_E=3.0^\circ$, *i.e.*, a defined wave number $q=6.18\times 10^5\ \text{m}^{-1}$. From a nonlinear regression, the values and expanded uncertainties ($k=2$) for τ_C are calculated and are also given in Fig. 1. Here and in all further measurements, no systematic deviations of the measured correlation function from Eq. 1 could be observed; see the lower part of Fig. 1.

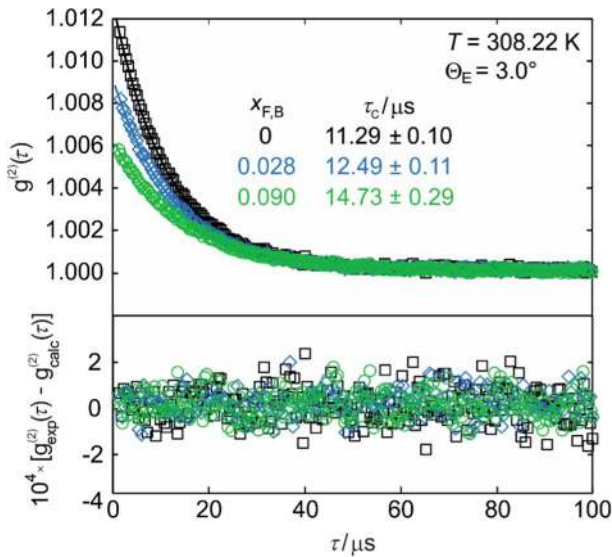


Fig. 1 Measurement examples of normalized correlation functions (upper part) and the residuals (lower part) for the binary mixtures of $[\text{C}_4\text{C}_1\text{Im}][\text{PF}_6]$ and $[\text{PFBMIm}][\text{PF}_6]$ with bulk mole fraction $x_{F,B}=0$ (squares), 0.028 (diamonds), and 0.090 (circles) as a function of the lag time τ at $T=308.22$ K, 0.1 MPa, and $\Theta_E=3.0^\circ$. The lines represent the fits according to Eq. 1

An increase in the concentration of the fluorinated IL is accompanied by an increase in the decay times of the surface fluctuations, which are clearly outside combined expanded uncertainties. At $x_F=0.028$, for example, τ_c is about 11 % larger than the value associated with the pure non-fluorinated IL $[\text{C}_4\text{C}_1\text{Im}][\text{PF}_6]$. According to the first-order approximation, $\tau_c \approx 2\eta/(\sigma q)$, which is a sound representation for the present fluids due to the relatively small reduced capillary numbers $Y \ll 0.145$ [48], increasing τ_c values with increasing $[\text{PFBMIm}][\text{PF}_6]$ mole fraction are most probably related to an increase in the viscosity and/or a decrease in the surface tension. The latter behavior can be expected taking into account that the fluorinated IL is enriched at the surface of the IL mixtures relative to the non-fluorinated one [30]. To resolve the separate influences of the liquid viscosity and surface tension on the dynamics of the surface fluctuations, it is necessary to combine the results from SLS with the surface tension data from the PD method in order to determine the viscosity.

For a reliable determination of viscosity, the dispersion relation for hydrodynamic surface fluctuations for a free liquid surface, *i.e.*, neglecting the presence of a second fluid phase, was solved in an exact manner [57, 58]. The assumption of a free liquid surface is reliably given for a system consisting of IL and argon at atmospheric pressure, where the density and viscosity of argon are distinctly smaller than the respective liquid quantities [44, 55]. Furthermore, the presence of viscoelastic effects and mono or double layers at the interface can be neglected for the studied systems. Besides the directly measured data for τ_c and q , reference values for the liquid density ρ and the surface tension σ are needed as input to solve the dispersion equation

[57, 58]. For ρ , the same correlations according to Eq. 2 or related predictions based on the measured densities were used as it has been performed in connection with the evaluation of the PD measurements. For σ , the T -dependent correlations, Eq. 3, developed in this work were applied for the temperature states investigated by SLS. Here, extrapolations of at most 6.0 K to the lowest temperature of 293 K studied by SLS were performed. Furthermore, the correlations for σ based on the data measured at $x_{\text{F,B}}=0.029$ were used to evaluate the SLS results obtained at $x_{\text{F,B}}=0.028$ due to the negligible difference in the compositions within combined uncertainties. To represent the final η values, the averages over six independent measurements at different wave numbers q of the surface fluctuations probed were calculated. The uncertainties for η were obtained from an error propagation based on the first-order approximation for τ_c . For this, the relative expanded uncertainties ($k=2$) associated with the primary measured variables $U_r(\tau_c)$ between (0.5 and 3.0) % and $U_r(q)=0.2$ % and with the reference data for the surface tension $U_r(\sigma)=4$ % were taken into account. Due to the good representation of the experimental data by the fits, the correlated σ data are assumed to have the same uncertainties as the measured ones. For the liquid dynamic viscosity η of the IL systems, a relative expanded uncertainty ($k=2$) of $U_r(\eta)=4.4$ % averaged over all studied states was obtained, which mainly originates from the uncertainty of the surface tension.

3 Results and Discussion

The measured results for the density, viscosity, and surface tension listed in the Supplementary Material (Tables S1 to S3) are discussed in the following subsections. Here, the influence of the fluorinated IL [PFBMIm][PF₆] on the bulk and surface properties of the studied binary IL mixtures of [C₄C₁Im][PF₆] and [PFBMIm][PF₆] is highlighted, and a prediction approach for the surface tension of binary IL mixtures considering their surface composition is proposed. A comparison of the properties measured in this study with experimental literature data has only been possible for [C₄C₁Im][PF₆] and is discussed below. Details about the source and number of the literature data as well as representations in form of deviation plots are provided in the Supplementary Material.

3.1 Density

The experimental data for the liquid mass densities ρ of the non-fluorinated and fluorinated ILs as well as their mixture at $x_{\text{F,B}}=0.028$ shown in the upper part of Fig. 2 were fitted as a function of temperature T by a second-order polynomial,

$$\rho_{\text{calc}}(T) = \rho_0 + \rho_1 T + \rho_2 T^2. \quad (2)$$

In the fitting, all data points were considered with the same statistical weight. Table 2 gives the fit parameters ρ_0 , ρ_1 , and ρ_2 and the average absolute deviations (AADs) of the experimental ρ data from the correlations based on Eq. 2.

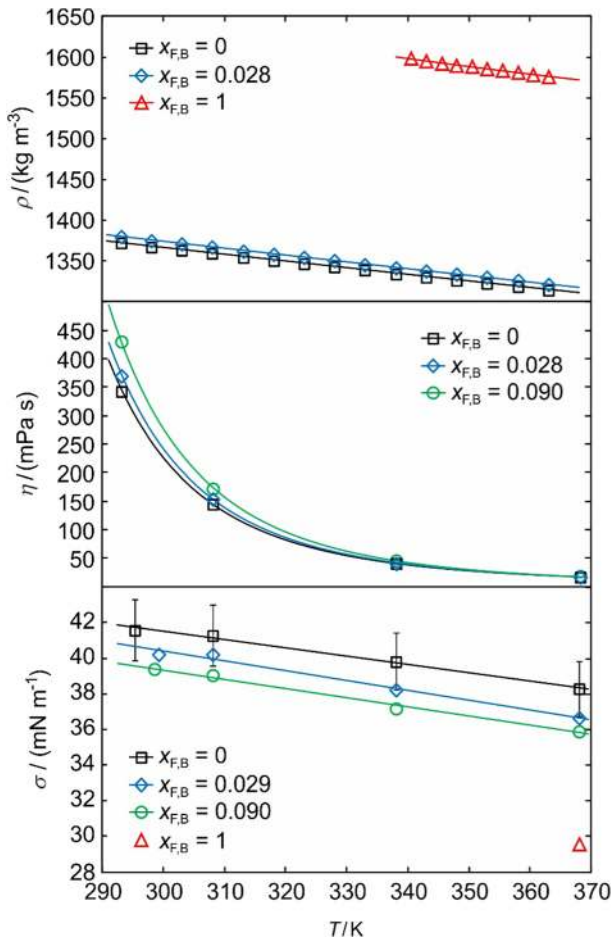


Fig. 2 Experimental data for density ρ (upper part), dynamic viscosity η (middle part), and surface tension σ (lower part) of the binary mixtures of $[\text{C}_4\text{C}_1\text{Im}][\text{PF}_6]$ and $[\text{PFBMIm}][\text{PF}_6]$ at 0.1 MPa including the correlations based on Eqs. 2, 3 and 4, respectively, as a function of temperature T for different bulk mole fractions $x_{\text{F,B}}$ of the fluorinated IL $[\text{PFBMIm}][\text{PF}_6]$. For the density and viscosity, error bars representing the expanded uncertainties ($k=2$) are within the symbols. For the surface tension, error bars of 4 % ($k=2$) are only shown exemplarily for one data set related to $x_{\text{F,B}}=0$ due to visibility purposes

For all three systems, decreasing densities with increasing temperature are found. Over the temperature range investigated, the fluorinated IL $[\text{PFBMIm}][\text{PF}_6]$ ($\rho \approx 1576 \text{ kg}\cdot\text{m}^{-3}$ at $T=363.15 \text{ K}$) shows about 20 % larger densities than the non-fluorinated IL $[\text{C}_4\text{C}_1\text{Im}][\text{PF}_6]$ ($\rho \approx 1314 \text{ kg}\cdot\text{m}^{-3}$ at $T=363.15 \text{ K}$). This can be related to the larger molecular weight of the fluorinated IL ($M=374.14 \text{ g}\cdot\text{mol}^{-1}$) compared to that of the non-fluorinated IL ($M=284.19 \text{ g}\cdot\text{mol}^{-1}$). Here, the light hydrogen atoms in the alkyl chain of the cation are substituted by heavier but still relatively small fluorine atoms, without having a strong impact on the molecular volume of the cation which is only slightly increased [29]. Increasing densities of pure ILs

by fluorination of the alkyl chains in the cations has also been reported by other authors [8, 29, 60]. A mole-based linear mixing rule for the molar volume of the mixtures, which is based on the densities of the pure substances correlated by Eq. 2 and assumes no excess molar volume, describes the correlated mixture densities for $x_{F,B}=0.028$ within 0.07 % between temperatures of (293.15 and 368.15) K. This finding that binary IL mixtures show negligible excess volume, in particular for ILs with different cations or anions of relatively similar sizes, is in agreement with literature [10, 15, 19, 20]. Thus, the linear mixing rule can also be applied to represent the mixture densities at $x_{F,B}=0.029$ studied with the PD method and at $x_{F,B}=0.090$ where no measurements could be performed in this work.

For pure $[C_4C_1Im][PF_6]$, the experimental density data reported in literature and mainly determined via vibrating-tube densimetry agree in most cases within combined uncertainties with our present measurement results based on Eq. 2, as can be seen in Fig. S1 of the Supplementary Material. The few large deviations between the different data sets of up to about 3 % seem not to be caused by differences in the water contents of the samples, but rather by different and/or undefined impurities, which can affect the density of ILs to this extent.

3.2 Viscosity

For the dynamic viscosity of the bulk phase of the IL systems studied, the temperature dependency of the experimental data obtained by SLS is represented by a Vogel-type equation,

$$\eta_{\text{calc}}(T) = \eta_0 \exp(B/(T - C)). \quad (3)$$

For the correlation, it was considered that the statistical weight of each experimental data point is the same. The fit parameters η_0 , B , and C and the AAD values of the measured η data from the correlations according to Eq. 3 are given in Table 3. In all cases, the absolute percentage residuals of the measured viscosity data from the fit, which are 0.53 % on average, are clearly smaller than the experimental expanded uncertainties.

The middle part of Fig. 2 shows that the viscosity of the three IL systems decreases strongly with increasing temperature, which is a common behavior of ILs [7]. With increasing mole fraction of the fluorinated IL up to 0.090, significantly increasing liquid viscosities are found. Comparing the results at $x_{F,B}=0.090$ with those at $x_{F,B}=0$, an increase in temperature results in smaller

Table 3 Coefficients of Eq. 3 for the liquid dynamic viscosity $\eta_{\text{calc}}(T)$ of the investigated IL systems at 0.1 MPa

System	$x_{F,B}$	$\eta_0/(\text{mPa}\cdot\text{s})$	B/K	C/K	AAD/ % ^a
$[C_4C_1Im][PF_6]$	0	0.11123	985.07	170.61	0.42
$[C_4C_1Im][PF_6]+[PFBMIm][PF_6]$	0.028 ± 0.001	0.084864	1058.8	166.90	0.26
$[C_4C_1Im][PF_6]+[PFBMIm][PF_6]$	0.090 ± 0.001	0.069838	1135.5	162.96	0.92

^aAverage absolute relative deviation between η and the correlation based on Eq. 3

relative changes in the η values from +25 % at 293 K down to +7.7 % at 368 K. Larger viscosities by adding a fluorinated IL to a non-fluorinated one were also reported by Merrigan *et al.* [25] who investigated different binary IL mixtures featuring a common $[\text{PF}_6]^-$ anion as well as non-fluorinated and fluorinated imidazolium-based cations of longer chain length than investigated here. This behavior also corresponds to larger viscosities found for ILs with fluorinated cations compared to their non-fluorinated analogues [8, 29].

In general, the viscosity of ILs is strongly governed by intramolecular entanglement as well as by intermolecular interactions including hydrogen bonding, electrostatic Coulomb interactions, dipole–dipole interactions, and van der Waals (vdW) interactions [7, 10]. Due to the complex interplay of such interactions over different spatial extensions, the bulk phase of ILs shows a distinct heterogeneity on a nanoscale in form of segregated colloid-like domains [7, 10, 31]. The polar domains mainly feature the anions and the charged head group of the cations as a result of attractive electrostatic interactions, while the nonpolar domains are formed by sufficiently long alkyl chains interacting predominantly via dispersive vdW forces [31].

By the introduction of fluorinated alkyl chains in ILs, a third segregated “fluorous” domain can be formed, as was observed for pure ILs in experiments [33] and MD simulations [28]. This so-called “fluorophobic” effect is caused by the exclusion of the fluorinated chains from other domains and especially from the nonpolar alkyl chains which show stronger vdW interactions between each other than to the fluorinated chains [61, 62]. Among the latter, rather weak or even repulsive interactions have been reported [62]. This behavior is apparently overcompensated by stronger attractive electrostatic cation–cation interactions induced by fluorinated cations than by non-fluorinated ones in the bulk of IL systems. The strongly negatively charged fluorine atoms in the fluorinated chains allow for a favorable electrostatic interaction with positively charged atoms in the imidazolium ring [29], which may also imply weak hydrogen bonding [61]. This results in stronger cation–cation interactions in $[\text{PFBMIm}][\text{PF}_6]$ than in $[\text{C}_4\text{C}_1\text{Im}][\text{PF}_6]$ as an additional contribution to the predominant anion–cation interactions. In conclusion, the more pronounced electrostatic interactions between the fluorinated cations than between the non-fluorinated ones seem to result in increased viscosities for pure $[\text{PFBMIm}][\text{PF}_6]$ and, thus, for the IL mixtures consisting of $[\text{PFBMIm}][\text{PF}_6]$ and $[\text{C}_4\text{C}_1\text{Im}][\text{PF}_6]$ relative to pure $[\text{C}_4\text{C}_1\text{Im}][\text{PF}_6]$. This is also reflected in the larger melting point of $[\text{PFBMIm}][\text{PF}_6]$ ($T_m \approx 339$ K) compared to $[\text{C}_4\text{C}_1\text{Im}][\text{PF}_6]$ ($T_m \approx 265$ K).

According to Fig. S2 in the Supplementary Material, the available experimental data for the viscosity of $[\text{C}_4\text{C}_1\text{Im}][\text{PF}_6]$ scatter around our data correlated by Eq. 3 with relative deviations between (+79 and –32) %. These deviations and those among the different data sets are often clearly outside combined measurement uncertainties, where our data from SLS seem to form the median of the literature data. Such large discrepancies, which have also been found for other ILs [55, 63, 64], may be attributed to the samples, especially the presence of water [38], and to the measurement procedure, where often conventional techniques

requiring a calibration procedure and/or the application of a macroscopic shear gradient are used.

3.3 Surface Tension

3.3.1 Summary and Discussion of Experimental Results

For the surface tension as characteristic macroscopic property of IL surfaces, the experimental data of the different IL systems determined by the PD method are described by a linear equation as a function of temperature,

$$\sigma_{\text{calc}}(T) = \sigma_0 + \sigma_1 T. \quad (4)$$

Besides the fit parameters σ_0 and σ_1 , the AAD values of the measured σ data from the correlations based on Eq. 4 are given in Table 4.

As can be seen from the lower part of Fig. 2, the surface tensions of the studied IL systems show the typical trend of decreasing values with increasing temperature. For all temperatures studied, the surface tension decreases with increasing mole fraction of the fluorinated IL. This behavior is in agreement with the significantly lower surface tension of the fluorinated IL [PFBMIm][PF₆] ($\sigma = 29.8 \text{ mN}\cdot\text{m}^{-1}$ at 368 K) compared to that of the non-fluorinated IL [C₄C₁Im][PF₆] ($\sigma = 38.3 \text{ mN}\cdot\text{m}^{-1}$ at 368 K). A significant reduction in the surface tension of pure ILs by fluorination of alkyl chains in cations [12] or anions [17] has also been found for other IL types. For the same binary IL mixtures as mentioned before in connection with the viscosity, Merrigan *et al.* [25] observed a distinct decrease in the surface tension of the mixtures relative to that of the non-fluorinated IL by adding small amounts of the fluorinated IL.

For the surface tension of [C₄C₁Im][PF₆] shown in Fig. S3 of the Supplementary Material, most of the literature data show positive deviations from the present data represented by Eq. 4. The deviations ranging between (+28 and -2) % are, however, often still within combined expanded uncertainties of the data sets, in particular considering the majority of the data sets which feature deviations of about 5 % and less. Differences in published surface tension data of ILs present in this work and in previous studies [55, 65] appear to be mainly caused by the underlying method and by impurities, out of which water as common impurity has no significant impact up to mole fractions of about 0.4 [38]. The tendency of somewhat lower σ values of the IL obtained in this study could also be seen

Table 4 Coefficients of Eq. 4 for the surface tension $\sigma_{\text{calc}}(T)$ of the investigated IL systems at 0.11 MPa

System	$x_{\text{F,B}}$	$\sigma_0/(\text{mN}\cdot\text{m}^{-1})$	$\sigma_1/(\text{mN}\cdot\text{m}^{-1}\cdot\text{K}^{-1})$	AAD/ % ^a
[C ₄ C ₁ Im][PF ₆]	0	55.46	-0.04649	0.27
[C ₄ C ₁ Im][PF ₆] + [PFBMIm][PF ₆]	0.029 ± 0.001	56.94	-0.05510	0.32
[C ₄ C ₁ Im][PF ₆] + [PFBMIm][PF ₆]	0.090 ± 0.001	54.87	-0.05173	0.29

^aAverage absolute relative deviation between σ and the correlation based on Eq. 4

for the reference fluids water and *n*-dodecane and is predominantly related to the calibration procedure and the evaluation of the droplet profile.

For ILs, the surface tension is often discussed in the context of the Langmuir's principle [66]. A comprehensive analysis of this principle can be found in the corresponding literature [10, 16, 67, 68]. In the following, only the information relevant for this study is given. Langmuir's principle [66] states that the surface tension is affected by the outer region of the surface. Since any fluid aims to reduce its surface energy and, thus, the surface tension, the segments of the IL with the lowest cohesive energy are preferentially enriched at the surface [16]. Besides this enthalpic effect, also entropic effects associated with the molecular orientation at the surface need to be considered [16]. For pure non-fluorinated ILs consisting of 1-*n*-alkyl-3-methylimidazolium ($[C_nC_1Im]^+$) cations and various types of anions, the alkyl side chains with their relatively weak vdW interactions align themselves preferentially towards the gas phase. This outer nonpolar layer is above an ionic sublayer mainly containing the charged head groups of the imidazolium rings and the anions, as could be evidenced in experiments [16, 30, 32] and MD simulations [16, 69]. In the study of Heller *et al.* [30], such behavior has also been observed by ARXPS measurements for the IL $[C_4C_1Im][PF_6]$ relevant in this work. For this IL, a slight enrichment of the relatively short butyl chain (C_4) and a slight depletion of the $[PF_6]^-$ anion is present at the outer surface region.

For pure imidazolium-based ILs with fluorinated chains in the cation [12, 30] or anion [17], these chains were also found to be strongly enriched at the surface. This enrichment is even larger than the enrichment of the alkyl chains, as it could be revealed by ARXPS for $[PFBMIm][PF_6]$ compared to $[C_4C_1Im][PF_6]$ [30]. The same behavior was also observed with MD simulations for pure ILs with fluorinated chains in the anions and alkyl chains in the cation, if the latter ones are relatively short [17]. The preferential enrichment of the fluorinated chains can mainly be related to the weaker intermolecular interactions between fluorinated chains compared to those between alkyl chains. In view of Langmuir's principle [66], the surface tension of $[PFBMIm][PF_6]$ is smaller than that of $[C_4C_1Im][PF_6]$, which is given by the PD measurement results at 368 K.

For binary mixtures of ILs with the same anion, but with non-fluorinated and fluorinated cations, experiments evidenced that the surface is preferentially occupied by the fluorinated chains [12, 30]. This includes the present mixture of $[C_4C_1Im][PF_6]$ and $[PFBMIm][PF_6]$, where ARXPS showed a clear enrichment of the fluorinated chains at the surface relative to the bulk composition, while the alkyl chains are depleted [30]. The relative enrichment of the fluorinated chains is more pronounced with decreasing mole fraction of $[PFBMIm][PF_6]$ and with decreasing temperature [30]. To analyze these structural effects in connection with the behavior of the surface tension, the measured σ data are shown in Fig. 3 as a function of the bulk mole fraction $x_{F,B}$ of $[PFBMIm][PF_6]$ for comparable temperatures. In all cases, the surface tension data show a significant decrease with increasing content of the fluorinated IL, which corresponds with the surface enrichment effects found by ARXPS qualitatively well. The somewhat larger

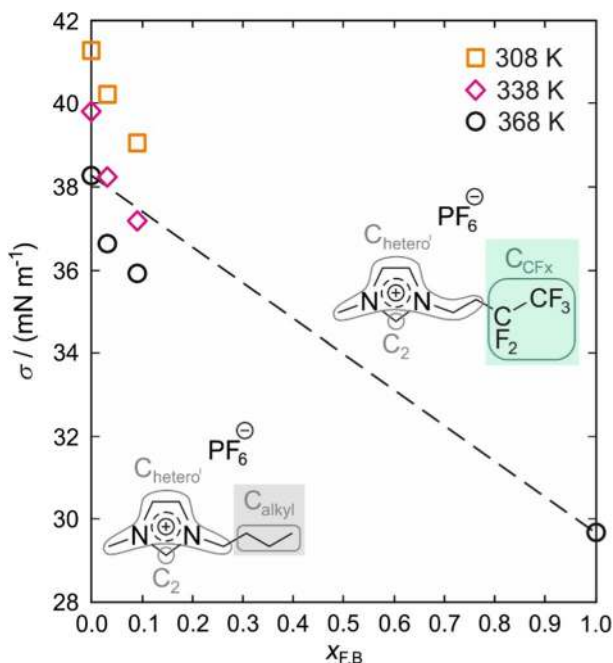


Fig. 3 Experimental surface tensions σ of the binary IL mixtures of $[\text{C}_4\text{C}_1\text{Im}][\text{PF}_6]$ and $[\text{PFBMIm}][\text{PF}_6]$ obtained by PD method as a function of the bulk mole fraction $x_{F,B}$ of the fluorinated IL $[\text{PFBMIm}][\text{PF}_6]$ at comparable temperatures. For 368 K, a linear mole fraction-based mixing rule using the surface tension data of the pure ILs is also shown as dashed line. For the two IL molecules given in the graph, the same nomenclature has been applied as in Ref. [30]. Errors bars for the surface tension data are not shown due to visibility purposes

enrichment at lower temperatures is not reflected in a more distinct decrease of the surface tension data, which is similar for the different temperatures studied.

3.3.2 Prediction Method for IL Mixtures

To quantify the effect of the surface enrichment on the surface tension, it is of interest to probe correlations between these microscopic and macroscopic properties of IL surfaces. In a recent approach [16], experimental ARXPS results were combined with MD simulations to represent the surface tension values of the homologous series of $[\text{C}_n\text{C}_1\text{Im}]^+$ -based ILs by contributions from different segments terminating the surface, considering their volume fractions. For binary IL mixtures being of interest here, different theoretical and empirical approaches have been discussed in the literature, as it has been reviewed by, *e.g.*, Smoll *et al.* [12] and Nakajima *et al.* [70]. A comparison with relevant approaches is not possible for the present IL mixture due to the lack of required input information. Instead, a new, phenomenological approach based on the surface tensions of the

pure ILs and their “effective” surface concentrations is suggested in the present work, which is shown in the following.

It is obvious that a relation between the experimental σ values and the bulk mole fractions in the IL mixtures fails. The discrepancy can be seen from the trend of the two measured surface tension results of the IL mixtures at 368 K which are systematically lower than the values predicted by a linear mixing rule based on the bulk mole fractions and the surface tensions of the pure ILs (see dashed line in Fig. 3). This non-ideal behavior has also been found by, *e.g.*, Smoll *et al.* [12] for binary IL mixtures with a common anion and two non-fluorinated $[C_nC_1Im]^+$ cations of different alkyl chain lengths ($n=2$ and 12). All this indicates that instead of bulk compositions, surface compositions need to be considered in appropriate prediction schemes [12, 70].

With the objective of developing a relatively simple relationship between surface tension and surface composition, we make use of the detailed structural information about the surface gained by ARXPS. This technique provides the quantitative

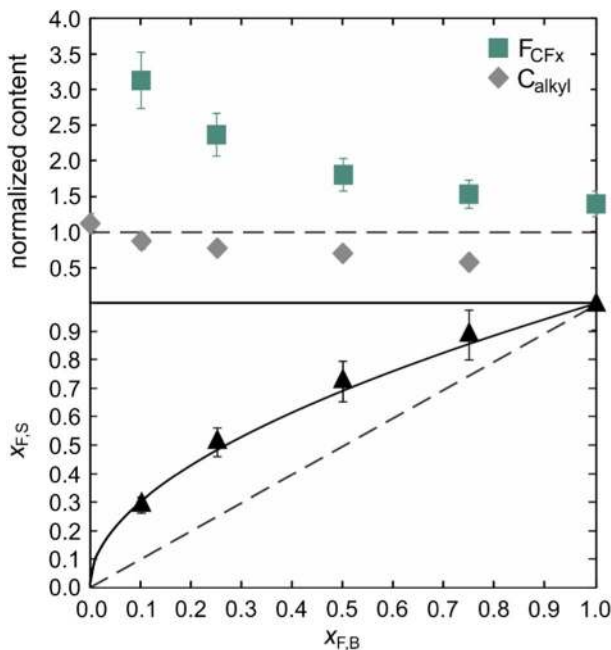


Fig. 4 Upper part: normalized F_{CFx} (squares) and C_{alkyl} (diamonds) contents at the outer surface measured by ARXPS at an emission angle of 80° [30] and the corresponding nominal contents (dashed line) of the binary IL mixtures of $[C_4C_1Im][PF_6]$ and $[PFBMIm][PF_6]$ at 368 K as a function of the bulk mole fraction $x_{F,B}$ of the fluorinated IL $[PFBMIm][PF_6]$. Lower part: mole fraction of the fluorinated chain at the surface, $x_{F,S}$, associated with the fluorinated IL $[PFBMIm][PF_6]$ obtained from the fit for the enrichment factors E_F (solid line) as a function of $x_{F,B}$ including the underlying $x_{F,S}$ values at $x_{F,B}=0.10, 0.25, 0.50, 0.75$, and 1.0 derived from Eq. 5 on the basis of the ARXPS results (triangles). For comparison, also the corresponding nominal stoichiometric contents (diagonal dashed line) are shown. The uncertainties for the normalized contents and for $x_{F,S}$ with values of 10 % are shown as errors bars

determination of the mole fractions of all elements typically found in ILs except for hydrogen. Using an emission angle of 80° with respect to the surface normal, the information depth is (1.0 to 1.5) nm, *i.e.*, the outer surface region is probed [34, 71]. By normalizing the measured content of each element in the outer surface region to the corresponding nominal content which corresponds to the bulk composition, so-called normalized contents can be calculated, which show relative enrichment (value > 1) or depletion (value < 1) in the outer surface region. For the mixtures of $[\text{C}_4\text{C}_1\text{Im}][\text{PF}_6]$ and $[\text{PFBMIm}][\text{PF}_6]$ studied at 368.15 K, the upper part of Fig. 4 shows the normalized contents of the fluorine atoms F_{CF_x} attached to carbon atoms C_{CF_x} in the fluorinated cation (shown in green color in Fig. 3) and of the carbon atoms C_{alkyl} in the alkyl chain of the non-fluorinated cation (shown in gray color in Fig. 3) as a function of the bulk mole fraction $x_{\text{F,B}}$, as they are reported in Ref. [30]. In this work, three significant digits were used for the corresponding measured contents contributing to the normalized contents. In addition, the uncertainty of the measured contents of 10 % [30] is assigned to the normalized contents.

In line with the previous discussion, a clear surface enrichment of the fluorinated chains is found, while the alkyl chains are depleted at the surface; see the upper part of Fig. 4a. Only for the pure non-fluorinated IL, *i.e.*, at $x_{\text{F,B}} = 0$, the C_{alkyl} group exhibits a slight enrichment. Furthermore, the normalized contents for the atoms in the $[\text{PF}_6]^-$ anion and in the imidazolium ring (not shown in the upper part of Fig. 4) are similar and close to 1 over the entire composition range, which indicates no distinct surface enrichment or depletion of both groups [30]. Thus, among the four relevant molecular segments in the IL mixtures, *i.e.*, the anion, the imidazolium ring, the alkyl chain, and the fluorinated chain, it is the idea of considering only the two competing, most surface-active moieties in form of the F_{CF_x} atoms in the fluorinated group and the C_{alkyl} group associated with the fluorinated and non-fluorinated IL, respectively. The mole fractions of these groups in such a pseudo-binary mixture account for their molar composition in the surface-near region and are considered to reflect the “effective” contributions of each associated IL to the surface tension of the IL mixture.

Based on the normalized F_{CF_x} and C_{alkyl} surface contents measured by ARXPS under an emission angle of 80° at 368.15 K for varying $x_{\text{F,B}}$ values, the surface mole fraction $x_{\text{F,S}}$ of the fluorinated chain associated with the fluorinated IL,

$$x_{\text{F,S}} = \frac{\text{norm. content}(F_{\text{CF}_x}) \cdot x_{\text{F,B}}}{\text{norm. content}(F_{\text{CF}_x}) \cdot x_{\text{F,B}} + \text{norm. content}(C_{\text{alkyl}}) \cdot (1 - x_{\text{F,B}})}, \quad (5)$$

can be derived analytically. Given the larger normalized content of F_{CF_x} than that of C_{alkyl} , Eq. 5 provides always larger values for $x_{\text{F,S}}$ than for $x_{\text{F,B}}$. The relative surface exposure of the fluorinated chain can be specified by an “enrichment factor” $E_{\text{F}} = x_{\text{F,S}}/x_{\text{F,B}}$, which shows a similar concentration-dependent trend as the normalized F_{CF_x} content and ranges between 2.9 at $x_{\text{F,B}} = 0.10$ and 1.0 at $x_{\text{F,B}} = 1.0$. Based on the E_{F} values at $x_{\text{F,B}} = 0.10, 0.25, 0.50, 0.75,$ and 1.0 calculated from Eq. 5 with the aid of the ARXPS results from the upper part of Fig. 4 [30], a simple empirical fit according to $E_{\text{F}} = a_{\text{F}} + b_{\text{F}} \cdot x_{\text{F,B}}^{-0.5}$ with the parameters $a_{\text{F}} = 0.10$ and $b_{\text{F}} = 0.90$ was performed. With this fit and Eq. 5, the surface mole fraction $x_{\text{F,S}}$ can be calculated

as a function of the bulk mole fraction $x_{F,B}$, which is shown by the solid line in the lower part of Fig. 4. As can be seen, the fit represents the underlying data points indicated by the triangles well and within the uncertainty of 10 % for the $x_{F,S}$ data, which is also associated with the normalized contents in Eq. 5. For relatively low $x_{F,B}$ values which are of main interest here, an initial strong deviation of $x_{F,S}$ from the nominal stoichiometric contents (see dashed diagonal line) is found. For the mixtures investigated at 368 K, the values for $x_{F,B}$ of 0.029 and 0.090 correspond to larger values of $x_{F,S}$ of 0.16 and 0.28, respectively. The compositions for the pure ILs, *i.e.*, at $x_{F,B}=0$ and 1, are not affected because the corresponding $x_{F,S}$ values are the same.

As a result, a surface mole fraction-based, linear mixing rule for the representation of the surface tension of the binary IL mixtures according to

$$\sigma = x_{F,S}\sigma_F + (1 - x_{F,S})\sigma_{\text{non-F}} \quad (6)$$

is suggested. This rule is based on the surface tension of the pure fluorinated (σ_F) and non-fluorinated ($\sigma_{\text{non-F}}$) IL and their corresponding “effective” surface mole fractions $x_{F,S}$ and $(1 - x_{F,S})$, and can, thus, be understood within the concept of Langmuir [66]. Figure 5 shows that the experimental surface tension data for the mixtures at 368 K represented as a function of $x_{F,S}$ follow the linear mole fraction-based mixing rule Eq. 6 given by the solid line well. By converting the $x_{F,S}$ values to

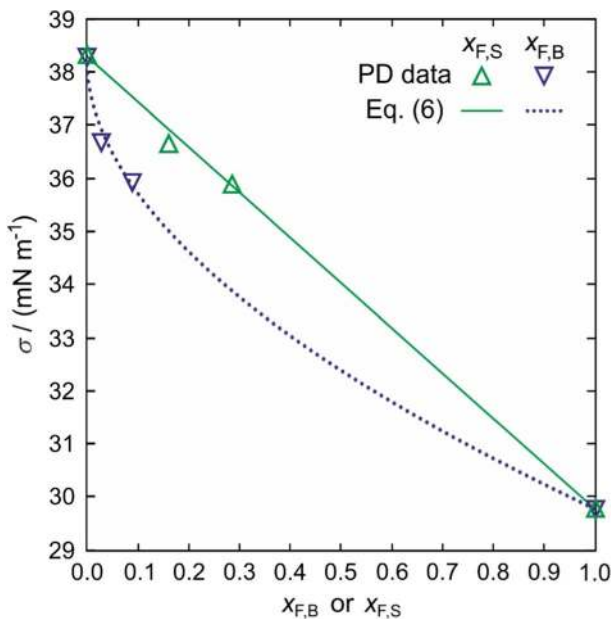


Fig. 5 Representation of the surface tensions σ obtained by the PD method (triangles up and down) and calculated by Eq. 6 (solid and dashed lines) for the binary IL mixtures of $[\text{C}_4\text{C}_1\text{Im}][\text{PF}_6]$ and $[\text{PFBMIm}][\text{PF}_6]$ at 368 K as a function of the bulk mole fraction $x_{F,B}$ or of the corresponding surface mole fraction $x_{F,S}$

corresponding $x_{F,B}$ values with the above fit for E , the σ values calculated by Eq. 6 can also be represented as a function of the bulk mole fraction $x_{F,B}$ in Fig. 5. These calculated σ values illustrated by the dotted line describe the experimental data and the expected convex behavior as a function of composition well.

The results for the surface tension and surface composition can also be discussed in the concept of the Gibbs adsorption equation [72]. This equation describes the excess of the surface-active compound, *i.e.*, the fluorinated IL [PFBMIm][PF₆], per unit area of the surface relative to the amount which would be present in case the corresponding bulk concentration is extended to the surface. Assuming an infinite dilution of the fluorinated IL in the binary mixtures where its activity coefficient approaches unity, the relative excess Γ_F at constant temperature T and pressure p is given by [72].

$$\Gamma_F = -\frac{x_{F,B}}{R \cdot T} \left(\frac{\partial \sigma}{\partial x_{F,B}} \right)_{T,p}, \quad (7)$$

where R is the ideal gas constant. To calculate the partial derivative in Eq. 7, the model for the surface tension in Eq. 6 was combined with the fit for E_F which connects $x_{F,S}$ with $x_{F,B}$. For the two studied mole fractions $x_{F,B}$ of 0.029 and 0.09 at 368 K, the corresponding Γ_F values are about (0.22 and 0.40) $\mu\text{mol}\cdot\text{m}^{-2}$. Positive Γ_F values indicate that the fluorinated IL with the lower surface tension is the surface-active substance and reduces the surface tension of the mixture. This is in accordance with the behavior of the experimental surface tensions and the predominant presence of the fluorinated IL observed by the ARXPS measurements [30].

To test the predictive character of Eq. 6 over a wider composition range, the surface tensions and surface compositions for binary mixtures of the non-fluorinated ILs [C₂C₁Im][Tf₂N] and [C₁₂C₁Im][Tf₂N] with the common [Tf₂N]⁻ (bis(trifluoromethylsulfonyl)imide) anion measured by Smoll *et al.* [12] at about 296 K were used. For this, the reported values for the relative surface exposure of the surface-active dodecyl chains in [C₁₂C₁Im]⁺, which is larger compared to the corresponding shorter ethyl chains in [C₂C₁Im]⁺, correspond to the surface mole fractions required in Eq. 6. For the 13 different mixture compositions ranging from pure [C₂C₁Im][Tf₂N] to pure [C₁₂C₁Im][Tf₂N], agreement between the experimental surface tensions [12] and the σ values calculated by Eq. 6 with an average absolute deviation of 0.8 % was found. All this indicates that the use of the surface mole fraction associated with the characteristic surface-active groups of each IL seems to be a reasonable parameter to describe the surface tension in binary mixtures of ILs containing a common anion via Eq. 6. Since this molar surface concentration is directly accessible by, *e.g.*, ARXPS, it may be of advantage in comparison to commonly used surface volume or area concentrations of IL molecules (see in Refs. [12, 70]) which can hardly be determined.

4 Conclusions

The present study contributes to an improved understanding of the surface tension and viscosity of binary mixtures of fluorinated and non-fluorinated ILs. Our work was not only motivated by the lack of detailed information about the thermophysical properties of such mixtures [25], but also by the question how the macroscopic properties viscosity and surface tension are influenced by the distinct structural organization in the bulk and at the surface of ILs containing fluorinated and non-fluorinated alkyl chains [17, 28, 30]. In this context, surface enrichment effects of the fluorinated IL [PFBMIm][PF₆] in its mixtures with the structurally similar, non-fluorinated IL [C₄C₁Im][PF₆] could recently be observed by ARXPS [30]. This binary mixture served as model system for the here-presented investigations by the PD method and SLS, both of which are non-invasive measurement techniques and rely on rigorous working equations. For the determination of the dynamic viscosity of the bulk liquid phase, the information about the dynamics of overdamped surface fluctuations probed by SLS at macroscopic thermodynamic equilibrium was combined with the surface tension data obtained by the PD method. For the studied temperatures between (293 and 368) K and [PFBMIm][PF₆] bulk mole fractions of 0, 0.03, and 0.09, the experimental viscosities and surface tensions of the IL mixtures show a distinct increase and decrease relative to the pure [C₄C₁Im][PF₆], which clearly reflects the underlying microscopic effects. Increasingly stronger electrostatic interactions between the fluorinated cations accompanied by the possible formation of fluorinated colloid-like nanodomains [17] seem to be responsible for larger viscosities in the IL mixtures with increasing [PFBMIm][PF₆] content. The distinct drop in the surface tension by adding only small amounts of fluorinated IL is in agreement with the surface enrichment effects of the fluorinated chain of [PFBMIm][PF₆] which shows a distinctly lower surface tension than [C₄C₁Im][PF₆]. By using the detailed microscopic information accessible by ARXPS, a new, phenomenological approach for the surface tension of the studied IL mixtures was suggested. Based on a linear mixing rule considering the surface tensions of the pure ILs and the surface mole fractions of the corresponding most surface-active group of each IL, *i.e.*, the fluorinated and non-fluorinated chain, good agreement between the correlated and experimental surface tensions was found. Despite its reasonable representation for the present binary IL mixture and for a further one consisting of two non-fluorinated ILs [12], the relatively simple approach suggested in this work, Eq. 6, requires further validation by application to other IL mixtures over broad ranges of composition and temperature, which is intended in our future activities. Furthermore, the present contribution may stimulate further research, where the usage of IL mixtures including, *e.g.*, fluorinated ILs serves as a promising way to tailor the surface and bulk properties for specific applications related to surface and colloid chemistry.

Acknowledgments Open Access funding provided by Projekt DEAL. This work was financially supported by the German Research Foundation (Deutsche Forschungsgemeinschaft, DFG). H.-P. S. thanks the European Research Council (ERC) under the European Union's Horizon 2020 research and innovation programme for financial support, in the context of the Advanced Investigator Grant "ILID" to H.-P. S. (Grant Agreement No. 693398-ILID). The authors thank Bettina Heller and Ulrike Paap from the

Institute of Physical Chemistry II of the Friedrich-Alexander-University Erlangen-Nürnberg (FAU) for the analysis of the samples by angle-resolved X-ray photoelectron spectroscopy.

Open Access This article is licensed under a Creative Commons Attribution 4.0 International License, which permits use, sharing, adaptation, distribution and reproduction in any medium or format, as long as you give appropriate credit to the original author(s) and the source, provide a link to the Creative Commons licence, and indicate if changes were made. The images or other third party material in this article are included in the article's Creative Commons licence, unless indicated otherwise in a credit line to the material. If material is not included in the article's Creative Commons licence and your intended use is not permitted by statutory regulation or exceeds the permitted use, you will need to obtain permission directly from the copyright holder. To view a copy of this licence, visit <http://creativecommons.org/licenses/by/4.0/>.

References


1. H.H. Lin, J.D. Peng, V. Suryanarayanan, D. Velayutham, K.C. Ho, J. Power Sources **311**, 167–174 (2016)
2. M. Bidikoudi, L.F. Zubeir, P. Falaras, J. Mater. Chem. A **2**, 15326–15336 (2014)
3. A. Weiß, M. Munoz, A. Haas, F. Rietzler, H.-P. Steinrück, M. Haumann, P. Wasserscheid, B.J.M. Etzold, ACS Catal. **6**, 2280–2286 (2016)
4. J. Joni, M. Haumann, P. Wasserscheid, Adv. Synth. Catal. **351**, 423–431 (2009)
5. S. Katsuta, Y. Yoshimoto, M. Okai, Y. Takeda, K. Bessho, Ind. Eng. Chem. Res. **50**, 12735–12740 (2011)
6. B. Sasikumar, G. Arthanareeswaran, A.F. Ismail, J. Mol. Liq. **266**, 330–341 (2018)
7. P. Wasserscheid, T. Welton, *Ionic Liquids in Synthesis* (Wiley-VCH, Weinheim, 2007)
8. A.B. Pereiro, J.M.M. Araújo, S. Martinho, F. Alves, S. Nunes, A. Matias, C.M.M. Duarte, L.P.N. Rebelo, I.M. Marrucho, A.C.S. Sustain. Chem. Eng. **1**, 427–439 (2013)
9. M.L. Ferreira, M.J. Pastoriza-Gallego, J.M.M. Araújo, J.N. Canongia Lopes, L.P.N. Rebelo, M.M. Piñeiro, K. Shimizu, A.B. Pereiro, J. Phys. Chem. C **121**, 5415–5427 (2017)
10. H. Niedermeyer, J.P. Hallett, I.J. Villar-Garcia, P.A. Hunt, T. Welton, Chem. Soc. Rev. **41**, 7780–7802 (2012)
11. G. Chatel, J.F.B. Pereira, V. Debbeti, H. Wang, R.D. Rogers, Green Chem. **16**, 2051–2083 (2014)
12. E.J. Smoll Jr., M.A. Tesa-Serrate, S.M. Purcell, L. D'Andrea, D.W. Bruce, J.M. Slattery, M.L. Costen, T.K. Minton, K.G. McKendrick, Faraday Discuss. **206**, 497–522 (2018)
13. W.A. Wakeham, A. Nagashima, J.V. Sengers, *Measurement of the Transport Properties of Fluids—Experimental Thermodynamics* (Blackwell Scientific Publications, Oxford, 1991)
14. A.I. Rusanov, V.A. Prokhorov, *Interfacial Tensiometry* (Elsevier, Amsterdam, 1996)
15. M.T. Clough, C.R. Crick, J. Grasvik, P.A. Hunt, H. Niedermeyer, T. Welton, O.P. Whitaker, Chem. Sci. **6**, 1101–1114 (2015)
16. K. Shimizu, B.S.J. Heller, F. Maier, H.-P. Steinrück, J.N. Canongia Lopes, Langmuir **34**, 4408–4416 (2018)
17. A. Luís, K. Shimizu, J.M.M. Araújo, P.J. Carvalho, J.A. Lopes-da-Silva, J.N. Canongia Lopes, L.P.N. Rebelo, J.A.P. Coutinho, M.G. Freire, A.B. Pereiro, Langmuir **32**, 6130–6139 (2016)
18. T.M. Koller, C. Steininger, M.H. Rausch, A.P. Fröba, Int. J. Thermophys. **38**, 167 (2017)
19. M. Chakraborty, T. Ahmed, R.S. Dhale, D. Majhi, M. Sarkar, J. Phys. Chem. B **122**, 12114–12130 (2018)
20. J.N. Canongia Lopes, T.C. Cordeiro, J.M.S.S. Esperança, H.J.R. Guedes, S. Huq, L.P.N. Rebelo, K.R. Seddon, J. Phys. Chem. B **109**, 3519–3525 (2005)
21. M. Montanino, M. Moreno, F. Alessandrini, G.B. Appetecchi, S. Passerini, Q. Zhou, W.A. Henderson, Electrochim. Acta **60**, 163–169 (2012)
22. G. Annat, M. Forsyth, D.R. MacFarlane, J. Phys. Chem. B **116**, 8251–8258 (2012)
23. P. Navia, J. Troncoso, L. Romani, J. Chem. Eng. Data **52**, 1369–1374 (2007)
24. J.J. Fillion, J.F. Brennecke, J. Chem. Eng. Data **62**, 1884–1901 (2017)
25. T.L. Merrigan, E.D. Bates, S.C. Dorman, J.H. Davis Jr., Chem. Commun. **2000**, 2051–2052 (2000)
26. M.B. Oliveira, M. Domínguez-Pérez, M.G. Freire, F. Llovel, O. Cabeza, J.A. Lopes-da-Silva, L.F. Vega, J.A. Coutinho, J. Phys. Chem. B **116**, 12133–12141 (2012)

27. M.B. Oliveira, M. Domínguez-Pérez, O. Cabeza, J.A. Lopes-da-Silva, M.G. Freire, J.A.P. Coutinho, J. Chem. Thermodyn. **64**, 22–27 (2013)
28. A.B. Pereira, M.J. Pastoriza-Gallego, K. Shimizu, I.M. Marrucho, J.N. Canongia Lopes, M.M. Piñeiro, L.P. Rebelo, J. Phys. Chem. B **117**, 10826–10833 (2013)
29. G.D. Smith, O. Borodin, J.J. Magda, R.H. Boyd, Y. Wang, J.E. Bara, S. Miller, D.L. Gin, R.D. Noble, Phys. Chem. Chem. Phys. **12**, 7064–7076 (2010)
30. B.S.J. Heller, M. Lexow, F. Greco, S. Shin, G. Partl, F. Maier, H.-P. Steinrück, Chem. Eur. J. **26**, 1117–1126 (2020)
31. J.N. Canongia Lopes, A.A.H. Pádua, J. Phys. Chem. B **110**, 3330–3335 (2006)
32. K.R.J. Lovelock, C. Kolbeck, T. Cremer, N. Paape, P.S. Schulz, P. Wasserscheid, F. Maier, H.-P. Steinrück, J. Phys. Chem. B **113**, 2854–2864 (2009)
33. Y. Shen, D.F. Kennedy, T.L. Greaves, A. Weerawardena, R.J. Mulder, N. Kirby, G. Song, C.J. Drummond, Phys. Chem. Chem. Phys. **14**, 7981–7992 (2012)
34. K.R.J. Lovelock, I.J. Villar-Garcia, F. Maier, H.-P. Steinrück, P. Licence, Chem. Rev. **110**, 5158–5190 (2010)
35. F. Maier, J.M. Gottfried, J. Rossa, D. Gerhard, P.S. Schulz, W. Schwieger, P. Wasserscheid, H.-P. Steinrück, Angew. Chem.-Int. Edit. **45**, 7778–7780 (2006)
36. C. Kolbeck, N. Paape, T. Cremer, P.S. Schulz, F. Maier, H.-P. Steinrück, P. Wasserscheid, Chem. Eur. J. **16**, 12083–12087 (2010)
37. M. Lexow, B.S.J. Heller, G. Partl, R.G. Bhui, F. Maier, H.-P. Steinrück, Langmuir **35**, 398–405 (2019)
38. A.P. Fröba, P. Wasserscheid, D. Gerhard, H. Kremer, A. Leipertz, J. Phys. Chem. B **111**, 12817–12822 (2007)
39. J. Canny, IEEE Trans. Pattern Anal. Mach. Intell. **8**, 679–698 (1986)
40. I. Bucher, Circle fit (<https://www.mathworks.com/matlabcentral/fileexchange/5557-circle-fit>), MATLAB Central File Exchange. Accessed 24 Mar 2020
41. F.K. Hansen, G. Rødsrud, J. Colloid Interf. Sci. **141**, 1–9 (1991)
42. W. Wagner, A. Pruss, J. Phys. Chem. Ref. Data **31**, 387–535 (2002)
43. E.W. Lemmon, M.L. Huber, Energy Fuels **18**, 960–967 (2004)
44. E.W. Lemmon, I.H. Bell, M.L. Huber, M.O. McLinden, *REFPROP, Standard Reference Data Program, version 10.0* (National Institute of Standards and Technology, Gaithersburg, 2018)
45. International Association for the Properties of Water and Steam, “Revised Release on Surface Tension of Ordinary Water Substance,” IAPWS R1-76, June 2014. (<http://www.iapws.org/relguide/Surf-H2O.html>)
46. A. Mulero, I. Cachadiña, M.I. Parra, J. Phys. Chem. Ref. Data **41**, 043105 (2012)
47. C. Tegeler, R. Span, W. Wagner, J. Phys. Chem. Ref. Data **28**, 779–850 (1999)
48. A.P. Fröba, S. Will, Light Scattering by Surface Waves - Surface Light Scattering, in *Experimental Thermodynamics Advances in Transport Properties of Fluids*, vol. IX, ed. by M.J. Assael, A.R.H. Goodwin, V. Vesovic, W.A. Wakeham (Royal Society of Chemistry, Cambridge, 2014), pp. 22–35
49. A.P. Fröba, *Simultane Bestimmung von Viskosität und Oberflächenspannung transparenter Fluide mittels Oberflächenlichtstreuung* (Friedrich-Alexander-University Erlangen-Nürnberg, Doctoral thesis, Erlangen, 2002)
50. A.P. Fröba, A. Leipertz, Int. J. Thermophys. **22**, 41–59 (2001)
51. T. Klein, S. Yan, J. Cui, J.W. Magee, K. Kroenlein, M.H. Rausch, T.M. Koller, A.P. Fröba, J. Chem. Eng. Data **64**, 4116–4131 (2019)
52. T.M. Koller, T. Klein, C. Giraudet, J. Chen, A. Kalantar, G.P. van der Laan, M.H. Rausch, A.P. Fröba, J. Chem. Eng. Data **62**, 3319–3333 (2017)
53. M.H. Rausch, L. Kretschmer, S. Will, A. Leipertz, A.P. Fröba, J. Chem. Eng. Data **60**, 3759–3765 (2015)
54. T.M. Koller, T. Prucker, J. Cui, T. Klein, A.P. Fröba, J. Colloid Interf. Sci. **538**, 671–681 (2019)
55. A.P. Fröba, H. Kremer, A. Leipertz, J. Phys. Chem. B **112**, 12420–12430 (2008)
56. A.P. Fröba, A. Leipertz, J. Chem. Eng. Data **52**, 1803–1810 (2007)
57. D. Langevin, *Light Scattering by Liquid Surfaces and Complementary Techniques* (Marcel Dekker, New York, 1992)
58. E.H. Lucassen-Reynders, J. Lucassen, Adv. Colloid Interface Sci. **2**, 347–395 (1970)
59. T.M. Koller, J. Ramos, P.S. Schulz, I.G. Economou, M.H. Rausch, A.P. Fröba, J. Phys. Chem. B **121**, 4145–4157 (2017)
60. J.E. Bara, C.J. Gabriel, T.K. Carlisle, D.E. Camper, A. Finotello, D.L. Gin, R.D. Noble, Chem. Eng. J. **147**, 43–50 (2009)

61. R. Berger, G. Resnati, P. Metrangolo, E. Weber, J. Hulliger, Chem. Soc. Rev. **40**, 3496–3508 (2011)
62. M. Yano, T. Taketsugu, K. Hori, H. Okamoto, S. Takenaka, Chem. Eur. J. **10**, 3991–3999 (2004)
63. B. Hasse, J. Lehmann, D. Assenbaum, P. Wasserscheid, A. Leipertz, A.P. Fröba, J. Chem. Eng. Data **54**, 2576–2583 (2009)
64. T. Koller, M.H. Rausch, P.S. Schulz, M. Berger, P. Wasserscheid, I.G. Economou, A. Leipertz, A.P. Fröba, J. Chem. Eng. Data **57**, 828–835 (2012)
65. T.M. Koller, M.H. Rausch, J. Ramos, P.S. Schulz, P. Wasserscheid, I.G. Economou, A.P. Fröba, J. Phys. Chem. B **117**, 8512–8523 (2013)
66. I. Langmuir, Chem. Rev. **6**, 451–479 (1930)
67. C. Kolbeck, J. Lehmann, K.R.J. Lovelock, T. Cremer, N. Paape, P. Wasserscheid, A.P. Fröba, F. Maier, H.-P. Steinrück, J. Phys. Chem. B **114**, 17025–17036 (2010)
68. T.M. Koller, M.H. Rausch, K. Pohako-Esko, P. Wasserscheid, A.P. Fröba, J. Chem. Eng. Data **60**, 2665–2673 (2015)
69. H.F. Almeida, M.G. Freire, A.M. Fernandes, J.A. Lopes-da-Silva, P. Morgado, K. Shimizu, E.J. Filipe, J.N. Canongia Lopes, L.M. Santos, J.A. Coutinho, Langmuir **30**, 6408–6418 (2014)
70. K. Nakajima, M. Lísal, K. Kimura, Surfaces of Ionic Liquids, in *Surface and Interface Science: Liquid and Biological Interfaces*, vol. 7, ed. by K. Wandelt (Wiley, Weinheim, 2020), pp. 351–389
71. H.-P. Steinrück, Phys. Chem. Chem. Phys. **14**, 5010–5029 (2012)
72. J.W. Gibbs, *The Scientific Papers of J. W. Gibbs* (Dover Publications, Mineola, 1961)

Publisher's Note Springer Nature remains neutral with regard to jurisdictional claims in published maps and institutional affiliations.

Affiliations

Thomas M. Koller¹  · **Frances D. Lenahan**¹ · **Patrick S. Schmidt**¹ · **Tobias Klein**¹ · **Julian Mehler**² · **Florian Maier**³ · **Michael H. Rausch**¹ · **Peter Wasserscheid**^{2,4} · **Hans-Peter Steinrück**³ · **Andreas P. Fröba**¹

✉ Thomas M. Koller
thomas.m.koller@fau.de

¹ Institute of Advanced Optical Technologies – Thermophysical Properties (AOT-TP), Department of Chemical and Biological Engineering (CBI) and Erlangen Graduate School in Advanced Optical Technologies (SAOT), Friedrich-Alexander-University Erlangen-Nürnberg (FAU), Paul-Gordan-Straße 8, 91052 Erlangen, Germany

² Institute of Chemical Reaction Engineering (CRT), Department of Chemical and Biological Engineering (CBI), Friedrich-Alexander-University Erlangen-Nürnberg (FAU), Egerlandstraße 3, 91058 Erlangen, Germany

³ Chair of Physical Chemistry II, Department of Chemistry and Pharmacy, Friedrich-Alexander-University Erlangen-Nürnberg (FAU), Egerlandstraße 3, 91058 Erlangen, Germany

⁴ Forschungszentrum Jülich, Helmholtz-Institute Erlangen-Nürnberg for Renewable Energy (IEK 11), Egerlandstraße 3, 91058 Erlangen, Germany